



Application of effective elastic media models for pore system evaluation of Albian grainstone carbonates from Campos Basin, Brazil

Irineu de A. Lima Neto, Roseane M. Misságia, Marco A. R. de Ceia and Nathaly L. Archilha.

Laboratório de Engenharia e Exploração de Petróleo (LENEP) – Universidade Estadual do Norte Fluminense (UENF)

Copyright 2013, SBGF - Sociedade Brasileira de Geofísica

This paper was prepared for presentation during the 13th International Congress of the Brazilian Geophysical Society held in Rio de Janeiro, Brazil, August 26-29, 2013.

Contents of this paper were reviewed by the Technical Committee of the 13th International Congress of the Brazilian Geophysical Society and do not necessarily represent any position of the SBGF, its officers or members. Electronic reproduction or storage of any part of this paper for commercial purposes without the written consent of the Brazilian Geophysical Society is prohibited.

Abstract

Carbonate reservoirs have great economic significance at worldwide. Carbonates represent a significant portion of the Brazil's deepwater oil production, whose importance has increased with new discoveries in the post-salt and pre-salt oil deposits. In contrast to the sandstones, often carbonates display a complex pore structure with a wide range of pore sizes and shapes, which are characterized by a heterogeneous pore system. This study aims to research grainstone post-salt carbonate samples (Albian-age) of the offshore Campos Basin, Brazil by laboratorial evaluation and rock physics models application to predict interparticle aspect ratio and quantitative fractions of dual pore system approach under ultrasonic and dry conditions. The goal is to estimate elastic moduli considering intergranular porosity expected to oncologic/oolitic grainstones by use of Effective Elastic Media (EEM) theory models: KT (Kuster-Toksöz), SC (Self-consistent) and DEM (Differential Effective Medium), and spherical or microporosity dominant inclusions. The Albian carbonate data set was evaluated in laboratory and pore aspect ratios were determined by comparing measured P- wave velocity data to EEM models. Thus, this study provides a methodology to predict intergranular porosity expected to oncologic/oolitic Albian grainstone carbonates, and characterizes the interparticle aspect ratio applying EEM models and a quantitative fraction of inclusions according to dual pore system approach under ultrasonic and dry conditions. The results allowed interparticle aspect ratio estimation and a quantitative impact of inclusions by EEM models application, and help us to understand the elastic properties of the Albian carbonates.

Introduction

The seismic reservoir monitoring is an important tool for oil production management. Mainly seismic characteristic changes are studied by direct impact: geomechanical framework, pore space and fluid saturation. Additionally, indirect factors such pressure and temperature have the potential to modify the elastic moduli. Estimation of reservoir properties for conventional siliciclastic systems has been an active area for several decades worldwide, including Brazil. However, carbonate rocks have great economic significance, about 60% of the world's oil

reservoirs. The carbonate reservoirs represent a significant portion of the Brazil's deep water oil production, whose importance has increased with new discoveries in the post-salt and pre-salt oil deposits. Thus, in contrast to sandstones, carbonates display a complex pore structure with a wide range of size and shape pores, characterized by a heterogeneous pore system (Wang, 2001; Baechle et al., 2007).

The siliciclastic rocks have mainly interparticle (intergranular) pores, while most carbonates contain a complex pore system such as moldic, vuggy, interparticle and intraparticle. The complex pore system makes the porosity-velocity relationship highly scattered and the pore type can cause about as 40% change in P-wave velocity for a given porosity, then pore shape appears to be the dominant factor in carbonate rock physics. Moldic, intraframe, and vuggy pores have a rounded trend and make the rock stronger causing higher seismic velocity compared to interparticle pores. However, thin or elongated pores such as cracks and microporosity often lead to slower velocity by rock softening (Xu and Payne, 2009; Oh and Spikes, 2012). The pore aspect ratio is a textural parameter that contributes for stiffness or softness carbonate rock characterization. Therefore, the relationship between pore shape and the elastic properties is important to be understood.

This work aims to study grainstone post-salt carbonate samples (Albian-age) of the offshore Campos Basin, Brazil, through laboratorial evaluation and rock physics models application to predict the interparticle aspect ratio and fractions of the dual pore system under ultrasonic and dry conditions.

Data Set

Albian carbonate reservoirs from Campos basin are located in southeastern Brazil, and into two megasequences: Shallow Carbonate platform (Early to Middle Albian), and Marine Transgressive Megasequence (Late Albian to Early Tertiary). Calcarenites and calcirudites form oil reservoirs in shallow water, which are composed mostly of grainstones and packstones containing oncolites, peloids, oolites and rare bioclasts. Calcarenites with matrix-free and oncolite/oolite-rich comprise the best reservoir facies showing porosities ranging between 20 and 34%, and permeabilities exceeding 100 mD (Bruhn et al., 2003).

The available samples in this work correspond with Early to Middle Albian. Thin section micrographs shown interparticle pore predominance and texture complexities and pore fabric (Figure 1), while laboratory petrophysical measurements of porosity, permeability and density are showed in the Table 2. A mineralogical characterization

was performed using X-ray diffractogram and Reitveld method, and results shown calcite predominance (Table 1). Grainstones of Well 1 exhibited better permeability, and grainstones of Well 2 presented more calcite cementation causing reduction of permeability (Table 2). The mineral moduli (Table 2) were built in order the percent weight shown in Table 1. P- and S-wave velocities were measured under dry and ultrasonic conditions using effective pressure equal 2.55 MPa avoiding transducers coupling noise and undesirable pore system impact with fractures induction.

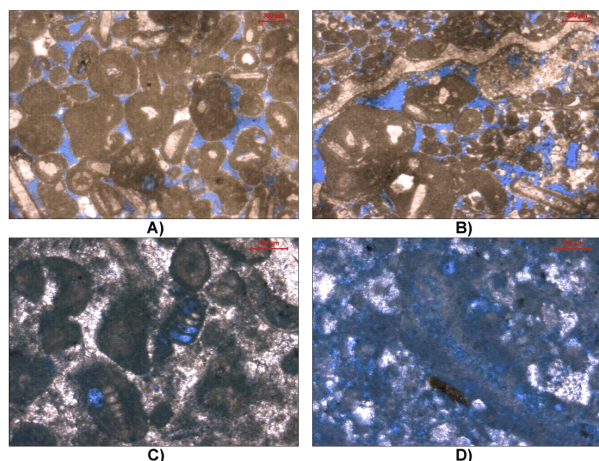


Figure 1: Thin sections taken from the core samples showing the complex texture and pore fabric. The main textures from core samples are oolitic grainstones: Well 1 (A and B) and Well 2 (C and D).

Methodology

Anselmetti and Eberli (1999) showed that carbonate rocks having intergranular and intercrystalline primary porosity. Inclusion of oomoldic, moldic and vugular porosities cause a positive deviation from P- and S-wave velocities and negative deviation by microporosity or fractures (Kumar and Han, 2005). Thus, pore aspect ratio estimation helps to determine stiffest or softest intervals and hydraulic fractured area. The aspect ratio (α) is related to pore shape in sedimentary rocks and effects caused on elastic properties. In this work, pore aspect ratios were determined by comparing measured velocities from Albian grainstone carbonate data to Effective Elastic Media (EEM) theory models: KT (Kuster-Toksöz), SC (Self-consistent) and DEM (Differential Effective Medium).

The goal is to estimate the elastic moduli for intergranular porosity expected for oncolytic/oolitic grainstones by use of EEM models and inclusions spherical or microporosity dominant. Thus, bulk (K) and shear (μ) modulus and ultimately P- and S-wave velocities can be estimated by EEM rock physics models. The pore aspect ratio is a textural parameter evaluated into the predominant dual pore system: 1) Interparticle or intercrystalline porosity, a reference expected to oncolytic/oolitic grainstones; and a second inclusion must express 2) Moldic, vuggy or spherical pore; or 3) Microporosity. The method was summarized in steps:

1- Prediction of Albian grainstones interparticle aspect ratio and assumption to be representative of the average aspect ratio. The Figure 2 shows a workflow to predict the interparticle aspect ratio as of Vp and mineralogical properties measured from grainstone samples. The aspect ratio is calibrated from 0.01 to 1 until the absolute error between measured and calculated Vp to be a minimum value. The laboratory input data set was measured under ultrasonic and dry conditions in accordance with EEM theories (Mavko et al., 2009).

2- Determination of dual pore system inclusions considering the interparticle aspect ratio predicted in the previous step and measured Vp, after then adjust of pore fraction phases for each EEM by spherical pore ($\alpha = 1$) or microporosity ($\alpha = 0.01$). Thereby, the interparticle inclusion was considered a reference for data set and we evaluated the second inclusion sphere or microporosity dominant by EEM adjust. The percent distribution of aspect ratio inclusions fitted for each model aiming correspondence with dry measured velocities and mineralogical properties evaluated for the data set. In Figure 3, we performed a flowchart to determine the dual pore system.

Sample	Weight %				
	Calcite	Dolomite	Quartz	Feldspar	Fluorite
W1-01	99.71	0.29	0.00	0.00	0.00
W1-02	95.20	0.92	2.13	1.76	0.00
W1-03	96.98	1.76	0.63	0.63	0.00
W1-04	96.47	0.52	1.46	1.55	0.00
W1-05	95.56	1.37	1.19	0.00	1.88
W1-06	95.50	2.49	0.89	0.00	1.12
W1-07	96.98	1.55	1.04	0.43	0.00
W2-01	99.81	0.00	0.20	0.00	0.00
W2-02	99.37	0.00	0.64	0.00	0.00
W2-03	98.77	0.85	0.38	0.00	0.00
W2-04	100.00	0.00	0.00	0.00	0.00

Table 1: The mineralogical characterization using X-ray diffractogram and Reitveld method.

Sample	ϕ (%)	k (mD)	Dry - ρ (g/cm ³)	Mineral			Dry - VP (km/s)	Dry - VS (km/s)
				K (GPa)	μ (GPa)	ρ (g/cm ³)		
W1-01	23.031	8.95	2.702	76.85	32.03	2.710	3.111	1.797
W1-02	25.713	221.50	2.688	74.65	31.86	2.709	2.973	1.745
W1-03	22.070	32.15	2.688	76.33	32.09	2.712	2.788	1.671
W1-04	22.277	13.50	2.702	75.10	31.80	2.709	3.191	1.942
W1-05	28.514	126.60	2.691	76.47	32.44	2.720	2.101	1.457
W1-06	28.881	602.30	2.699	76.76	32.47	2.719	2.257	1.490
W1-07	22.195	9.78	2.685	76.16	32.16	2.711	2.838	1.708
W2-01	16.317	0.24	2.696	76.68	32.02	2.710	4.107	2.358
W2-02	21.944	2.02	2.685	76.41	32.07	2.710	2.996	1.768
W2-03	19.720	0.81	2.691	76.71	32.13	2.711	2.639	1.644
W2-04	22.113	1.02	2.699	76.80	32.00	2.710	2.855	1.717

Table 2: Summary of acoustics and petrophysical data measured in the laboratory.

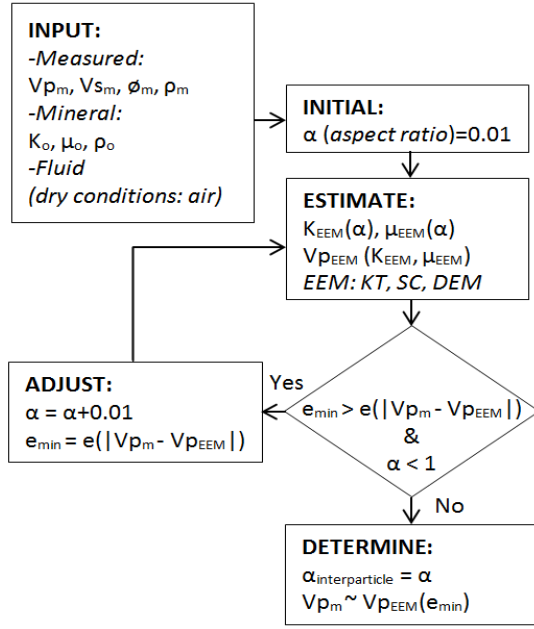


Figure 2: The workflow to predict the interparticle aspect ratio as of V_p measured from grainstone samples. The absolute error between the modeled and adjusted V_p was calculated aiming minimum value.

Theory

Effective Elastic Media (EEM) theories assume that separated pores and cracks may or may not be connected to each other (Berryman et al., 2002). We can predict the effective elastic moduli of a mixture of grains and pores specifying (1) the volume fractions of the various inclusions, (2) the elastic moduli of the various inclusions, and (3) the geometric details of inclusions arrange to each other (Mavko et al., 2009). In this case, a knowledge regarding the pore shape and characteristics of microstructures is necessary, but at every location in a formation is difficult. The Albian carbonate samples were evaluated to compose a data set with the necessary information to apply the EEM models and to determine the approximate complementary information of geometric details. Berryman (1980) gives expressions to P and Q for some inclusion shapes, and these terms are considered geometric factors by aspect ratio dependence.

Kuster-Toksöz (KT) model

Kuster and Toksöz (1974) derived expressions under ultrasonic frequency conditions to estimate the effective moduli K_{KT} and K_{KT} for a variety of the inclusions with dilute concentrations, additionally the geometric factors proposed by Berryman (1980), can be written as (Mavko et al., 2009):

$$(K_{KT}^* - K_m) \left(\frac{K_m + \frac{4}{3}\mu_m}{K_{KT}^* + \frac{4}{3}\mu_m} \right) = \sum_{i=1}^N x_i (K_i - K_m) P^{mi}$$

$$(\mu_{KT}^* - \mu_m) \left(\frac{\mu_m + \zeta_m}{\mu_{KT}^* + \zeta_m} \right) = \sum_{i=1}^N x_i (\mu_i - \mu_m) Q^{mi}$$

$$\zeta_m = \frac{\mu_m (9K_m + 8\mu_m)}{6(K_m + 2\mu_m)},$$

(1)

here, x_i is a volume concentration of porosity for N-phase composites, K_m and μ_m are bulk and shear moduli of host material, K_i and μ_i are bulk and shear moduli of the fluid inclusions, air properties for dry conditions.

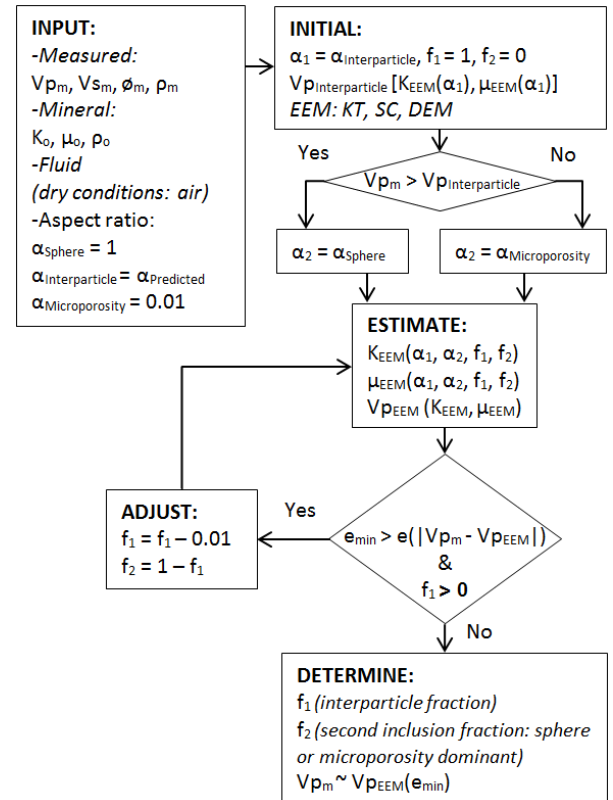


Figure 3: Determination of the dual pore system from fractions of the pore volume to interparticle (reference) and second EEM dominant inclusion (sphere or microporosity) by the EEM.

Self-consistent (SC) model

This method treats grains and pores symmetrically, requiring a single background material, grains and pores can be connected or disconnected depending on the porosity range. SC supposes a single inclusion

representing one of the components is embedded within a large surrounding matrix whose elastic properties are those of effective medium. The elastic properties of the solid grains and pores affect the elastic moduli of the rock. This model can incorporate multiple mineral phases for idealized ellipsoidal pores. The effective moduli (K_{SC}^* and μ_{SC}^*) of the infinite background matrix can be solved by iteration for N-phase composites, according to Equation 2 proposed by Berryman (1980) (Mavko et al., 2009).

$$\sum_{i=1}^N x_i (K_i - K_{SC}^*) P^{*i} = 0,$$

$$\sum_{i=1}^N x_i (\mu_i - \mu_{SC}^*) Q^{*i} = 0.$$
(2)

Differential Effective Medium (DEM) model

This model assumes isolated pores embedded in a host material that remains continuous at all porosities. DEM simulates porosities in a composite medium of two phases by incrementally adding small amounts of pores (phase 2) into a matrix (phase 1), until the total porosity (ϕ) is attained (Berryman, 1992):

$$(1 - \phi) \frac{d}{d\phi} [K^*(\phi)] = (K_2 - K^*) P^{*(2)}(\phi),$$

$$(1 - \phi) \frac{d}{d\phi} [\mu^*(\phi)] = (\mu_2 - \mu^*) Q^{*(2)}(\phi),$$
(3)

where, $K^*(0) = K_1$ and $\mu^*(0) = \mu_1$ are bulk and shear moduli of host material (phase 1), K_2 and μ_2 are bulk and shear moduli of the inclusions, the air properties for dry conditions.

Sample	Porosity (ϕ) %		Difference %
	Helium (He)	Mercury (Hg)	
W1-03	22.070	20.006	2.064

Table 3: A comparison between porosity calculated by different laboratorial methods.

Results

Prediction of the interparticle aspect ratio

The P-wave velocity of the grainstone samples measured under dry condition and mineralogical properties are input provided to the workflow (Figure 2). Figure 4 illustrates the result of the interparticle aspect ratio estimated from each sample, as the color map range indications. In addition, aspect ratio curve lines were plotted for calcite allowing comparison with impure samples. In Table 1, the calcite weight ranges from 95 to 100% of grainstone samples, and the solid red line represents the average aspect ratio ($\alpha=0.1$) for calcite, that able us to check a

good agreement for the low level of impurities (< 5%). Note that EEM models expressed different behaviors related to the interparticle aspect ratio, as expected by the particularities of each theory. All EEM models predicted interparticle aspect ratio for grainstone samples ranging from 0.05 to 0.15, with a mean acceptable value 0.1.

Determination of the dual pore system

After the interparticle aspect ratio prediction for each grainstone sample, it is necessary to determine the fractions of dual pore inclusions, see Figure 3. The sphere and microporosity aspect ratios are not known and were assumed according to Kumar and Han (2005). Figure 4 shows the sphere aspect ratio for carbonates generally ranges from 0.8 to 1.0, here it was assumed to be equal 1.0 due to similarities of values (dashed green line), and the microporosity aspect ratio was to be 0.01 (dashed cyan line).

The P-wave velocity measured versus porosity for dry carbonate samples were plotted (Figure 5). The calcite curve lines are plotted for each EEM model from interparticle reference ($\alpha=0.1$, solid red line), varying to spherical pore or microporosity. Then, dashed lines for different percentage of the spherical pore (blue lines) or microporosity (black lines) were plotted varying at each 10% of inclusion over interparticle line reference.

Iteratively, according to the Figure 3, fractions of dual inclusions were evaluated aiming to amount the Vp calculated by EEM models with Vp measured. Figure 6 shows the fraction results for each EEM model.

Comparing the dual fraction results of each EEM model in Figure 6, note that KT and DEM models tend to predict the most impact of the microporosity, where DEM expressed a slightly higher fraction. However, SC provided a significant spherical pore impact in dual pore system determination. In this investigation, we evaluated a grainstone sample available of Well 1 (W1-03) with mercury injection porosimeter, a destructive test. The result shows a difference ~2% (Table 3). The density of mercury allows evaluating mainly macro and mesopores while the helium macro, meso and micropores, then a difference was expected to get microporosity percent estimate. Therefore, the SC may be overestimating the spherical pore fractions, a similar problem described in Misaghi et al. (2010).

Conclusions

This research intended to provide a methodology to predict intergranular porosity expected to oncolytic/oolitic Albian grainstone carbonates, and characterizes the interparticle aspect ratio applying EEM models (KT, SC and DEM) and a quantitative fraction of inclusions according to dual pore system approach under ultrasonic and dry conditions.

The previous knowledge of the mineralogy, porosity, texture and complexities of microstructure allows the EEM models application and represents the elastic properties of the carbonates. The Vp measured in the laboratory served directly to estimate the interparticle aspect ratio for

data set from Albian grainstone carbonates. After, the interparticle aspect ratios were used to estimate fractions of inclusions for each model according to dual pore system approach. The results assist us to understand the elastic properties of the Albian carbonates.

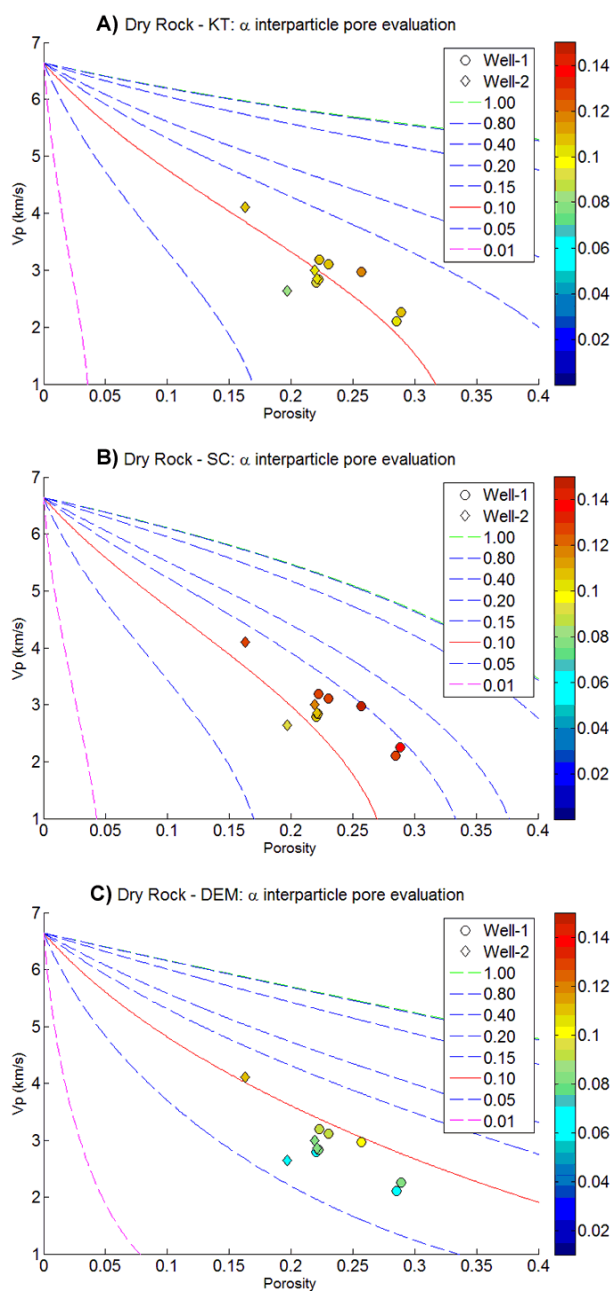


Figure 4: Interparticle pore evaluation using EEM models. The color bar shows the average aspect ratio estimated for each sample from Wells 1 and 2, in accordance with mineral properties (Tables 1 and 2), then the interparticle aspect ratio was assumed to oncolytic/oolitic grainstones (workflow in Figure 2). The calcite aspect ratio lines show the interparticle aspect ratio dominant next to 0.1 (solid red line, $\alpha=0.1$).

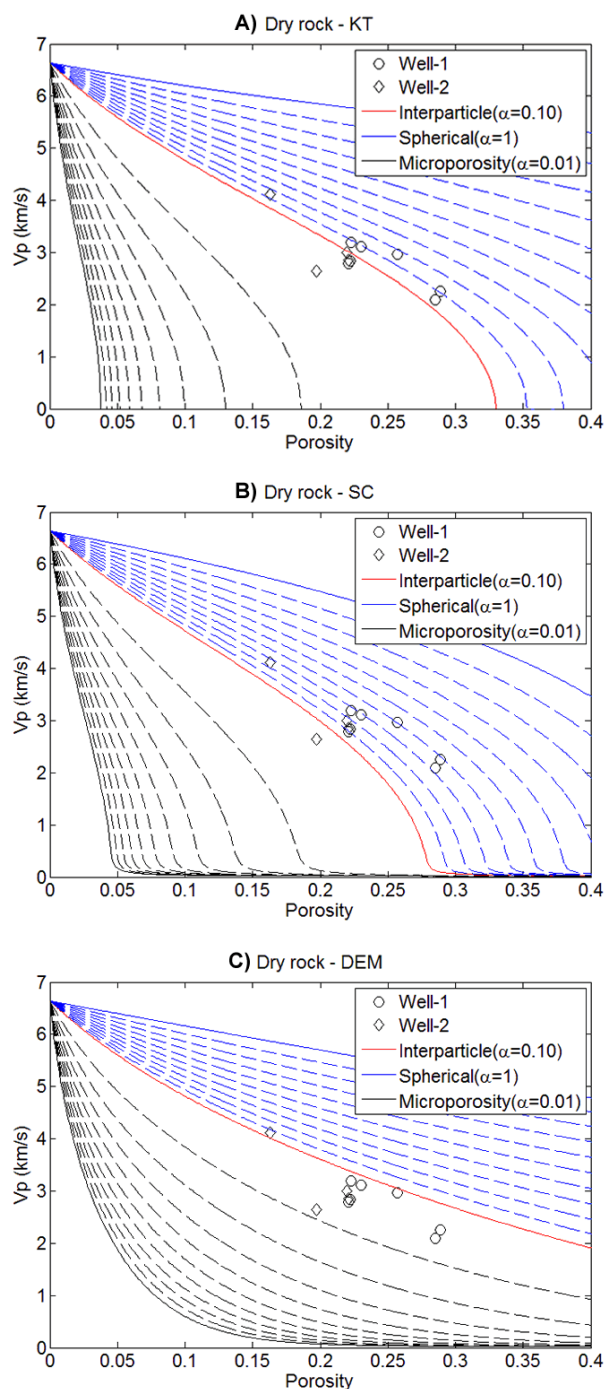


Figure 5: P-wave velocity versus porosity for dry carbonate samples for evaluation of the dual pore system using EEM models. The calcite dual pore system lines show the interparticle aspect ratio dominant next to 0.1 ($\alpha=0.1$, solid red line), and dashed lines for a different percentage of the spherical pore or microporosity, each 10% of inclusion over interparticle line reference.

We evaluate the pore system performing two porosity measurements: Helium gas and Mercury injection. The results shown a difference for porosity measured (Table 3). Helium gas measurement resulted in a higher value of porosity. Observed differences in porosity values reveal that Helium gas reached more microporosity than Mercury measurement. Thus, the KT and DEM can be suited to model the Albian grainstone carbonates. However, no model can be effectively recommended as the best model because the rock microstructure must be studied in details by evaluation of more available rock samples.

In future work, we will explore the analysis of digital images with multi-resolution μ CT aiming better evaluate the microporosity aspect ratio. This study can be supplemented by Gassmann's theory for fluid substitution.

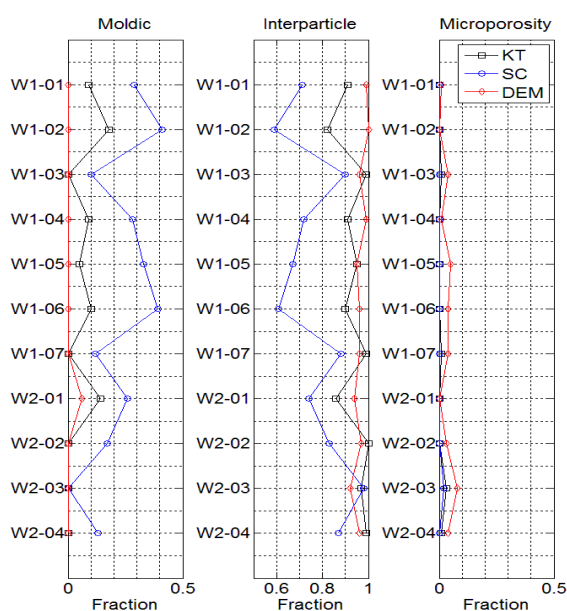


Figure 6: Comparison of fraction results between EEM models considering the interparticle aspect ratio estimated from Wells 1 and 2, a dual pore system balance for moldic (or spherical pore), interparticle and microporosity, see Figure 3.

Acknowledgments

The authors would like to thank UENF/LENP for the facilities provided to perform this work, ANP-PRH-20 and PETROBRAS for permission to use the data and to sponsor this study. IALN and NLA thank CAPES for their doctoral scholarships. RMM acknowledges FAPERJ for "Jovem Cientista" research grant.

References

Anselmetti, F.S., and G.P. Eberli, 1999, The velocity-deviation log: A tool to predict pore type and permeability trends in carbonate drill holes from sonic and porosity or density logs: *AAPG Bulletin*, **83**, 450–466.

Baechle, G.T., A. Colpaert, G.P. Eberli and R.J. Weger, 2007, Modeling velocity in carbonates using a dual porosity DEM model: 76th Annual International Meeting, SEG, San Antonio, Texas, 1589-1593.

Berryman, J.G., 1980, Long-wavelength propagation in composite elastic media, part 1: Spherical inclusions: *Journal of the Acoustical Society of America*, **68**, 1809-1819.

Berryman, J.G., 1992, Single-scattering approximations for coefficients in Biot's equations of poroelasticity: *Journal of the Acoustical Society of America*, **91**, 551-571.

Berryman, J.G., 1995, Mixture theory for rock properties, in T. J. Ahrens, ed., *Handbook of physical constants*: American Geophysical Union, 205-228.

Berryman, J.G., S.R. Pride, H.F. Wang, 2002, A differential scheme for elastic properties of rocks with dry or saturated cracks: *Geophysical Journal International*, **151**, 597-611. doi:10.1046/j.1365-246X.2002.01801.x.

Bruhn, C.H., J.A. Gomes, C.D. Lucchese Jr., and P.R. Johann, 2003, Campos basin: reservoir characterization and management – historical overview and future challenges, *Offshore Technology Conference*, OTC 15220, Houston, Texas, p. 1-14. doi: 10.4043/15220-MS.

Kumar, M., and D.H. Han, 2005, Pore shape effect on elastic properties of carbonate rocks: 75th Annual International Meeting, SEG, Expanded Abstract, **24**, 1477–1480.

Kuster, G.T., and M.N. Toksöz, 1974, Velocity and attenuation of seismic waves in two-phase media, Part I: Theoretical formulations: *Geophysics*, **39**, 587–606.

Mavko, G., T. Mukerji, and J. Dvorkin, 2009, *The rock physics handbook*, 2nd ed.: Cambridge University Press.

Misaghi A., S. Negahban, M. Landro, and A. Javaherian, 2010, A comparison of rock physics models for fluid substitution in carbonate rocks: *CSIRO publishing, Exploration Geophysics*, **41**, 146-154. <http://dx.doi.org/10.1071/EG09035>.

Oh, K.T., and K. Spikes, 2012, Velocity modeling to determine pore aspect ratios of the Haynesville shale: Expanded Abstracts of the 82nd Annual Meeting of the SEG, **31**, <http://dx.doi.org/10.1190/segam2012-0508.1>.

Wang, Z.Z., 2001, *Fundamentals of seismic rock physics*: *Geophysics*, **66**, 398-412.

Xu, S., and M.A. Payne, 2009, Modeling elastic properties in carbonate rocks: *The Leading Edge*, **28**, 66-74.